Experimental Investigation of Current Jumps in Linear Geometry Hot Cathode Ionization Gauges in Strong Magnetic Fields

Alberto Castillo Castillo[1,2,*], Felix Mackel[1], Michael Griener[1], Gregor Birkenmeier[1,2], the ASDEX Upgrade Team[1]

Abstract

In magnetic confinement nuclear fusion, neutral gas in the plasma edge region plays an important role for plasma fuelling and plasma wall interaction and thus influences the overall plasma behaviour. The ASDEX pressure gauge is a diagnostic instrument designed to provide local and temporally highly resolved measurements of the neutral gas flux density within the strong magnetic fields of fusion devices. It is a hot cathode ionization gauge with a linear geometry. Its function principle relies on the measurement of an ion current, caused by oscillating electrons in the gauge which ionize the neutral gas. Anomalous jumps in the ion current of up to 30% have been observed during gauge operation in the tokamak ASDEX Upgrade and the stellarator Wendelstein 7-X, which introduces an error in the measurement. This paper describes for the first time the characterization of these jumps over the broad operational space. Parameter dependencies on pressure, electron current, electrode potentials and magnetic field angle are discussed. The appearance of electrostatic oscillations with frequencies in the range of 160 – 350 MHz which are associated with the current jumps has been discovered. The frequency of these oscillations was found to scale with the oscillation frequency of the electron motion inside the gauge. Potential physical mechanisms to explain the jumps are discussed.

*Corresponding author
Email address: alberto.castillo@ipp.mpg.de (Alberto Castillo Castillo)
[1]Max Planck Institute for Plasma Physics, 85748 Garching, Germany
[2]Physik-Department E28, Technische Universität München, 85747 Garching, Germany

Keywords: Ionization gauge, Hot cathode, Current jumps, Instability, Two-stream instability, Fusion diagnostics
2010 MSC: 00-01, 99-00

1. Introduction

1.1. ASDEX Gauge

The amount of neutral gas in magnetic confinement fusion devices is an important parameter for their operation. In order to obtain high in-situ spatial and temporal resolution measurement of the neutral gas flux density, the ASDEX gauge was developed at the Max Planck Institute for Plasma Physics in Garching, Germany [1]. Due to their geometry, conventional ionization gauges such as the Bayard-Alpert gauge would not work correctly in the presence of magnetic fields. With magnetic flux densities in the order of 1 T or more, the trajectories of the electrons are confined to the magnetic field lines, with gyration radii smaller than 1 µm. Therefore, the ASDEX gauge is designed with a linear geometry aligned with the magnetic field. It is a hot cathode ionization manometer that can measure at neutral gas pressures in a wide range of $10^{-6} - 10^{-1}$ mbar, with a time resolution of up to 5 kHz[1] . These manometers are also in operation in the stellarator Wendelstein 7-X [2]. Similar gauges are planned for operation in ITER [3].

The working principle of the ionization gauge which is described in the following, is treated in more details in Ref. [1]. The ASDEX gauge is composed of 4 electrodes, whose positions and bias potentials are represented in Fig. 1(a). The electrons are thermionically emitted from the filament (Fil) at a potential of 70 V. It is made of a thorionated tungsten wire, heated by a direct electric current. The electrons are accelerated towards the acceleration grid (AG) - a grid of vertical wires biased at a high potential of 250 V. In between the filament and the grid there is the control electrode, which alternates between a low and high state of potential with a chopping frequency equal to the time resolution of the gauge. During its low state, electrons are prevented from passing

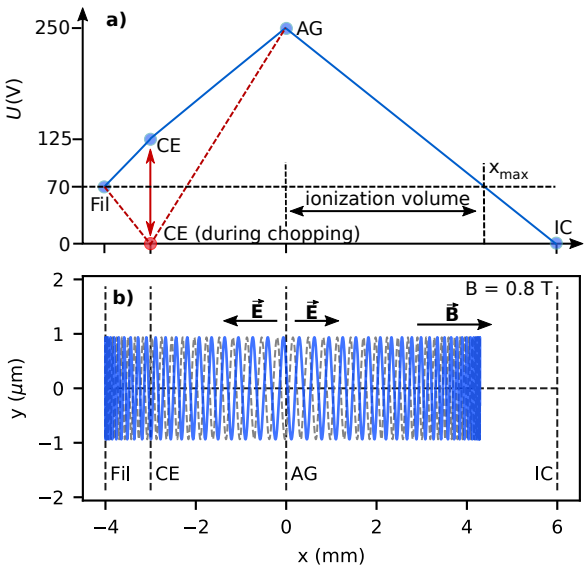

Figure 1: Electric potential along the electron trajectory in the gauge and the positions and potentials of the electrodes (a). 2D projection of an electron trajectory (blue continuous line as the electron moves in positive direction of x, and grey discontinuous when it is returning) (b).

through. Lastly, there is the ion collector (IC), a metal plate at ground potential that collects the produced ions within the ionization volume, leading to the ion current I_i.

In Fig. 1(b), the motion of the electrons along the gauge is represented. The portion of the electrons passes through the AG decelerates until they reach the point x_max where the electric potential is the same as in the filament. Then, they return towards the filament. If they experience no collisions, they have enough kinetic energy to be reabsorbed at the filament. However, if they loose any portion of their kinetic energy, they become trapped, oscillating back and forth the AG. Eventually they are absorbed at the AG, where the electron current I_e is measured.

The measurement of the neutral gas flux density F is calculated from the measurement of I_e and I_i with the formula given in Ref. [1] as:

$$F = \frac{I_\mathrm{i}}{(I_\mathrm{e} - I_\mathrm{i})\ d}, \tag{1}$$

where d is a sensitivity factor measured in calibration experiments, which is not constant, but varies for different values of F. Since the measurement is dependent on the currents, perturbations of these currents result in an error in the gauge measurement.

1.2. Current jumps

Sudden anomalous jumps in I_i are seen the pressure gauges of Wendelstein 7-X [4] and ASDEX Upgrade. The phenomenon observed in both machines are similar, even though there are differences in the design of the manometer. The gauges for Wendelstein 7-X use a straight LaB_6 filament, while the ones in ASDEX Upgrade use thoriated tungsten (0.4% ThO_2) 0.6 mm wire with a meander shape. Therefore, the occurrence of the current jumps is unlikely to be dependent on the material and shape of the filament, which implies a general physical process within the gauge is what causes the jumps. This physical mechanism is investigated for the first time in detail in this paper. As a typical example of the sudden jumps in I_i and I_e, two of these jumps are shown in fig. 2 at 5.9 s and 8.3 s. This measurement is taken during calibration at ASDEX Upgrade, where neutral gas is introduced at a constant rate up to a pressure of 3.3×10^{-3} mbar. In calibration shots, the toroidal field coils are energized (generating a toroidal magnetic flux density of $B_\mathrm{t} = 2.0\,\mathrm{T}$ at the vessel axis in this case). I_i would be expected to increase at a constant rate accordingly, but at these two points it experiences sudden jumps.

Examination of I_e in fig. 2(a) revealed perturbations on the electron current as well, simultaneous to the ones in I_i, visible in fig. 2(b). As the electron current is feedback controlled by changing the filament heating, it returns to the set value of 200 µA after the jumps. With no active control, I_e also stays on a modified level, as has been observed in laboratory conditions. As can be seen, the two jumps in I_i are of opposite sign, whereas the jumps of I_e go in the same

direction.

A detailed investigation of the behaviour of the jumps and the relevant parameter range where the occur can be found in the next section.

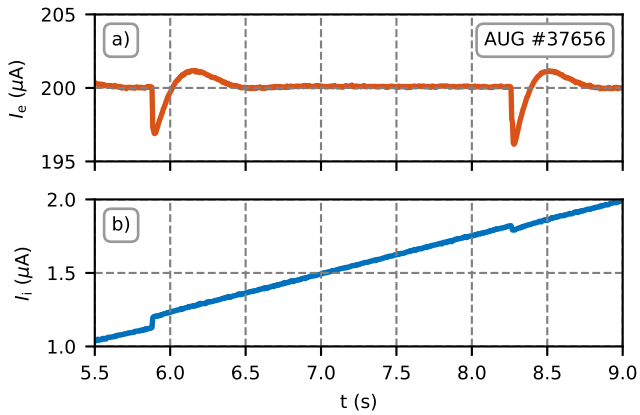

Figure 2: Electron (a) and ion (b) currents during manometer number 3 (bellow the divertor) of ASDEX Upgrade calibration presenting current jumps. Pressure range: 3.3×10^{-3} mbar.

2. Characterization of current jumps

2.1. Jump observed in ASDEX Upgrade operation

The current jumps observed in ASDEX Upgrade occur during plasma operation as well as during gauge calibration pulses with no plasma but with magnetic field and changing neutral pressure. These scenarios connect the measurement signals of the gauge in a pure way to the underlying neutral gas flux and are not disturbed by plasma events. Therefore, these pulses are an excellent scenario to provide an understanding of the general characteristics of these current jumps:

- **Ion current jumps**: The ion current can present sudden jumps and perturbations during the measurement. The jumps show a sudden increase or decrease of the current, which remains in a modified level afterwards. Analysis of the jumps detected in ASDEX Upgrade calibrations revealed an average amplitude of the jumps of $\pm 6.7\%$ of the total I_i reaching up to $\pm 40\%$ in rare cases.

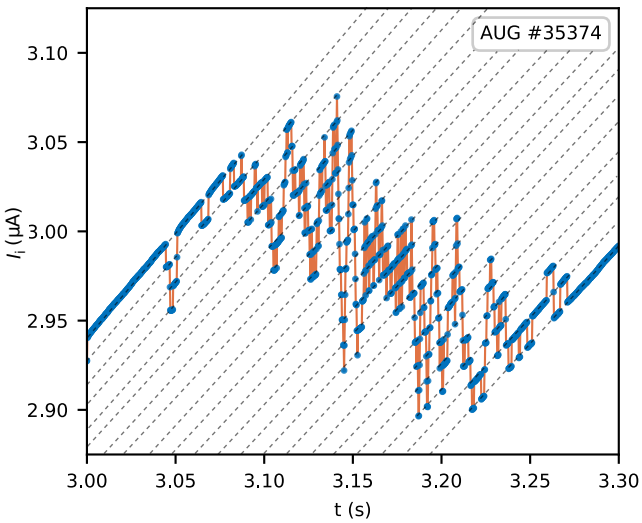

Figure 3: Ion current of manometer 5 (in pump chamber) of ASDEX Upgrade experiencing multiple jumps. The accumulation of data points in discrete lines shows a quantisation of the levels of current. The red line connects the data-points in chronological order. The dashed lines show all the same slope, corresponding to the pressure increase during this calibration pulse.

- **Electron current spikes**: Perturbations on I_e always appear simultaneously to the ion current jumps. They are smaller in amplitude than the jumps on I_i, with an average amplitude of $\pm 2.0\%$. Their sign is independent of the sign of the jumps in I_i, as exemplified in Fig. 2, and can be either positive or negative. The electron current returns later to its normal value after the spike due to the control of the heating current, even though the ion current remains in a modified state. In test done without active feedback control of the heating current, I_e also stays modified after the jumps.

- **Discrete number of current levels**: The ion current has been observed to jump between a discrete number of states. Typically, the jumps appear in pairs, with a jump followed by one opposite in sign that returns the current to its original state. In occasions, they appear in higher numbers, with the current jumping between multiple discrete levels. Fig. 3 shows an example of this behavior. This measurement was taken during calibra-

tion, with a constant increase of pressure. The ion current is expected to follow a straight slope, but instead experiences multiple jumps. The data points accumulate in discrete levels, each with a similar slope. This is an extreme example with 21 levels. Typically 2, 3 or 4 levels of current can be observed, with higher separation between the levels. In the particular case of Fig. 3, the separation between each level is relatively small, but added together, they represent a total change of 8.2% of the total I_{i}.

- **Jump occurrence rate**: In some occasions, the jumps consist of a single event, while in others the current experiences rapid jumps between discrete levels with high frequency. When the jump frequency is very high, the signal looks noisy, but consists of many jumps which can not be fully resolved as their frequency is in the same range as the time resolution of the gauge. The mean occurrence rate of single event jumps is $0.2\,\mathrm{s}^{-1}$ in the pressure range of $1\times10^{-5}-4.0\times10^{-3}$ mbar. Fig. 4 shows the currents during two similar calibration shots. Before 8 s, the ion current experiences some single event jumps. However, after t = 8 s, the current experiences fast jumps at rates similar to the time resolution of the gauges.
  Measurements in lab conditions proved the jumps can appear multiple times within each of the cycles of the chopping frequency (5 kHz). This gives a time scale for the jumps which is smaller than the time it takes for the gas to enter the gauge cover through the aperture (approximately 0.2 ms for H_2). Therefore, a real change in pressure is ruled out as a cause for the jumps. They also appear when a constant V_{CE} is used instead of an alternating one, so the chopping cycles are also discarded as a cause for the jumps.

2.2. Reproduction of ion current jumps in laboratory

The jumps observed during plasma and calibration pulses in tokamaks and stellarators were reproduced in laboratory conditions in order to study their dependency with multiple parameters. The experimental setup used is the same

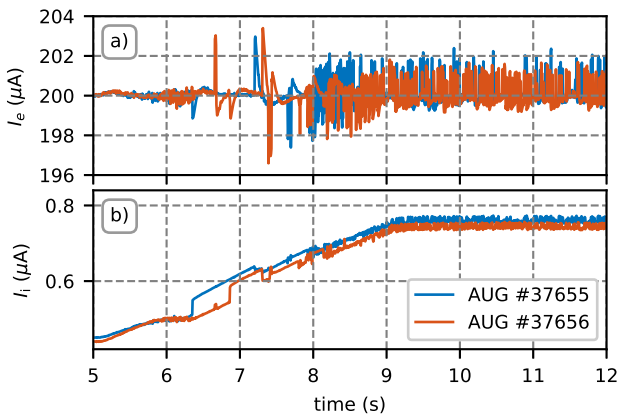

Figure 4: Electron (a) and ion (b) currents of manometer 1 (bellow divertor) of ASDEX Upgrade during two calibration shots with similar pressure time trace. Jumps in I_i with high occurrence rate appear after 8 s.

as described in Ref. [5], in which the gauge is placed in a vacuum chamber surrounded by an electromagnet. The electromagnet was used with magnetic field flux densities up to 0.8 T. The model of pressure gauges used for the experiments is the same currently in use at ASDEX Upgrade, with an ET4N (0.4% ThO_2) tungsten meander filament.

It was found that the ion current jumps could be reproduced by changing the value of I_e over time, instead of using the constant value of 200 µA. This produces current jumps with the same characteristics as the ones observed in ASDEX Upgrade gauges. Additionally, ion current jumps can also be reproduced by variation of the electrode potentials over time.

Under these controlled conditions, the dependency on I_e, electrode potential, magnetic field angle, and pressure were systematically tested, as described in the next section.

2.3. Parameter dependencies of current jumps

Dependencies of the jump behavior were discovered with four different parameters: electron current, neutral gas pressure, electrode potentials, and magnetic field angle. The ranges of values that were tested for each parameter are given in table 2 in the appendix. It is useful to distinguish between internal and

external parameters. The internal parameters, which are I_e and the electrode potentials, depend on the design and setup of the gauge, and therefore, can be adapted for a reliable operation. In contrast to this, the magnetic field angle and the pressure depend, as external parameters, on the operation of the fusion device.

The jumps can be reproduced by increasing or decreasing the value of I_e. Keeping all other parameters constant, the jumps appear at specific values of I_e. When using chopped V_{CE}, if the same increasing or decreasing ramp of I_e is repeated, the jumps in I_i appear always at the same value of the electron current. In experiments using a constant value of V_{CE}, the jumps appear at different values for increasing and decreasing I_e ramps, resulting in a hysteresis behavior. This hysteresis cycles can be observed in Fig. 5, where alternating cycles of increasing and decreasing I_e were used. I_i experiences jumps at different points depending on whether I_e is increasing or decreasing. In the example in the figure, I_e experiences a positive jump to a higher level and then a negative jump with increasing current, and a single positive jump at a smaller value of I_e when it is decreasing. The hysteresis cycles only appear with a continuous value of V_{CE}, presumably because when the chopping cycles are used, the system is resorted at the end of each cycle and thus, it can not retain information of its previous state. The rest of the experiments in this section correspond to chopped operation of V_{CE}, since it is the intended mode of operation of the gauge.

The reproducibility of ion current jumps at a specific value of I_e has been observed in all the cases when the same measurements have been repeated within the same day. However, this reproducibility does not necessarily last over longer periods. A possible reason for the lack of long-term reproducibility is the change over time of the emission properties of the filament. It is a known effect on other hot cathode ionization gauges that the spatial distribution of electron emission over the filament surface is unstable [6]. The long-term change in the reproducibility suggest that it is not the value of I_e itself which determines when

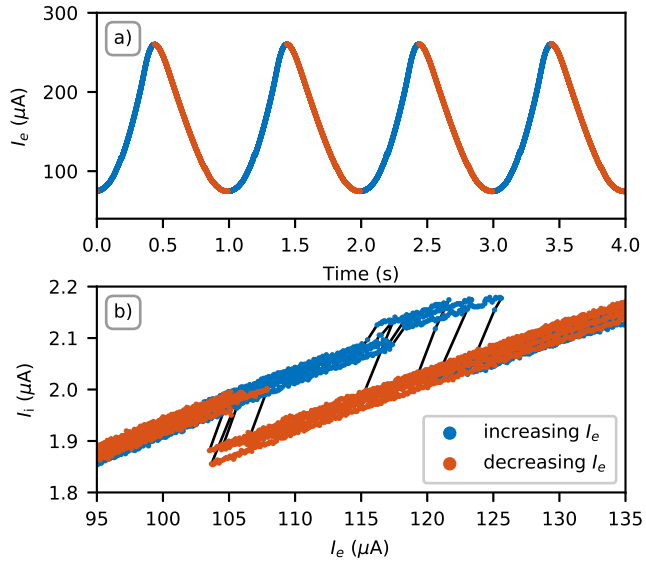

Figure 5: Electron current (a) during a laboratory measurement in which cycles of increasing and decreasing I_e were performed while keeping a constant CE voltage. (b) shows the value of the ion current as a function of the electron current.

the do the jumps occur, but a related parameter such as the electron density.

The characteristics of the current jumps are also influenced by the voltages of CE and AG. In order to test this dependency, multiple ramps of increasing I_e were done at different values of V_{AG} and V_{CE}. In each set of measurements a constant value was set for one of the two electrodes, while the other was incrementally increased in each of the I_e ramps. Fig. 6 shows 8 measurements, each corresponding to an I_e ramp taking 60 s with different values of V_{AG}. The figure represents the normalized ion current, which is the value used to calculate the flux density, as a function of I_e. It can be observed that the value of I_e at which the jumps appear is different for each value of V_{AG}. At the lower values of V_{AG}, there is only one jump that occurs at incrementally higher values of I_e as V_{AG} is increased. In the two curves with the highest potential, the current becomes unstable and experiences fast jumps between multiple levels of current The same is true for measurements with constant V_{AG} and different values of V_{CE}. The dependency of the jumps with the potential values is complex; a given

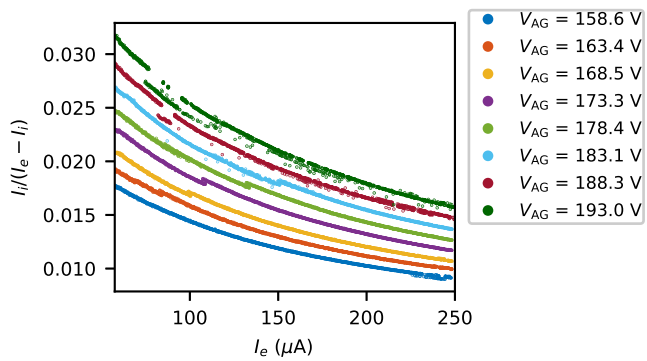

Figure 6: Normalized ion current as a function of I_e, corresponding to 8 measurements at different values of V_{AG}. V_{CE} is 130 V in all measurements.

jump may appear at linearly higher values of I_e with higher potential, but this relation can be inverse or non-linear for other jumps.

In Fig. 6, it can also be observed that the sensitivity of the gauge is strongly dependent on the electron current. If the sensitivity was constant with I_e, then all curves would be horizontal lines. This shows that the electron-to-electron interaction plays a role in the behavior of the gauge

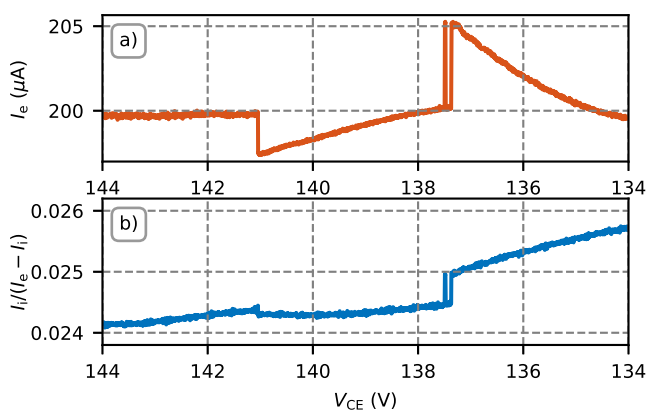

Figure 7: I_e (a) and normalized ion current (b) during an experiment in which V_{CE} is changed over time. Ion current jumps are observed during the V_{CE} ramp. V_{AG} is constant at 238.0 V and pressure is 1.2×10^{-3} mbar.

Experiments were also carried out in which V_{CE} and V_{AG} were changed over

time. The ion current jumps appear at specific values of the voltage, with short-term reproducibility. Fig. 7 shows the currents as a function of V_{CE} as it is being increased. The time interval shown in the figure corresponds to 0.3 s. In this example, it can be appreciated how the perturbations in I_{e} are temporary as the feedback returns it to the desired value, but the modification to I_{i} persists until the second jump happens. Similar behaviour can be observed by changing V_{AG}.

The dependency of the jumps on the pressure was observed during the gauge calibration at ASDEX Upgrade. In a given gauge, the jumps occur at similar value of pressures if the same pressure ramp is repeated. An example of this behavior can be observed in Fig. 4, where two identical pressure time trace were used, and the jumps appear at similar points in time with a similar structure. This dependency was also found in laboratory measurements of I_{e} ramps at different values of pressure. Fig. 8 shows an example of this dependency, with 6 different I_{e} ramps at different values of pressure. In the figure, the point of I_{e} at which the jumps happen changes with the pressure. A jump can be observed at all 6 measurements at an increasing value of I_{e} starting at 200 µA for the lowest pressure. In the 3 measurements with highest pressure values, additional jump appear also at lower values of I_{e}. This exemplifies a complex dependency of the jumps with the pressure, similar to the one shown with the electrode potential. This measurements were taken using H_2 as neutral gas, and with the standard electrode potentials as described in Fig. 1(a).

A total of 60 experiments, reproducing the same electron current ramp were carried out to test this dependency in the range of pressures of $5\times10^{-5}-1.2\times10^{-1}$ mbar. During these experiments no current jumps were observed at pressures over 6.7×10^{-2} mbar. This upper pressure limit has remained consistent in all others experiments done in the laboratory conditions, also with other configurations of electrode voltages.

Experiments were also done at the lowest achievable pressures in this setup, in the order of 10^{-8} mbar. At such low pressures there in not enough neutral

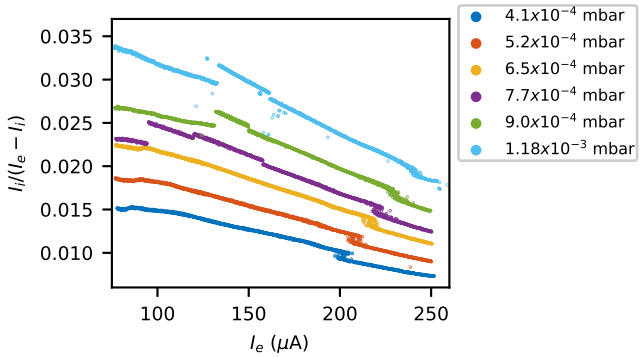

Figure 8: Normalized ion current as function of electron current during experiments in the laboratory in which the electron current is increased over time. The same experiment carried out at 6 different values of the neutral gas pressure are displayed.

gas particles for measurable ionization, so there is no measurement of the ion current. I_e ramps were carried out, and the spikes in the electron current were observed. Fig. 9 shows an example of the electron current perturbations during increasing and decreasing ramps of the heating current. Perturbations in the electron current can be observed when it descends bellow 120 µA, and at 140 µA when it is increasing. In this case the electron current is not feedback-controlled, so the perturbations persist, showing discrete levels of current. These perturbations have similar characteristics to the ones observed simultaneous to the ion current jumps and appear in a reproducible manner at similar value of I_e if the measurement is repeated. Thus, jumps in the ion current are only the symptom of the underlying process, which is caused by a change in the electron behavior. This gives a range of pressures at which the jumps occur of $<10^{-8} - 6.7 \times 10^{-2}$ mbar.

Another external parameter which is addressed in this analysis is the magnetic field angle α, which also influences the current jumps. α is defined as the angle between the main axis of the gauge (parallel to the electric field) and the magnetic field. This is a relevant parameters because, for fusion devices such as tokamaks, where there is a plasma current, generating a variable poloidal com-

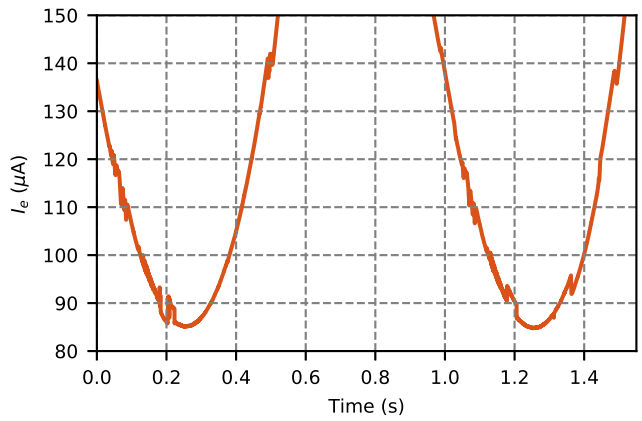

Figure 9: Electron current over time in a laboratory experiment in which I_e is increased and decreased in cycles. The pressure during the experiment was 1.2×10^{-7} mbar.

ponent of the magnetic field. Therefore, the gauges are not necessarily aligned with the magnetic field during operation. In tests during ASDEX Upgrade gauge calibration, a vertical component of the magnetic field was introduced using the poloidal field coils. This changed the magnetic field angles by up to $\alpha = \pm 2.9°$, and significantly modified the behaviour of the current jumps in some of the gauges.

This result motivated further studies in laboratory conditions. To this end, the same I_e ramps were repeated at angles between $-20°$ and $+20°$ with increments of $2°$. This is done using a mechanism in the gauge mount that allows to change the orientation of the gauge inside the electromagnet. The rotation axis is perpendicular to the base plate of the gauge. All measurements were done with the same value of the electrode potentials and at a pressure of 2.8×10^{-4} mbar. As seen in Fig. 10, the behaviour of the current and the current jumps changes significantly with even the introduction of a $4°$ angle. As can be seen in the figure, the current becomes unstable and experiences different jumps at different values of the angle.

There are two potential effects on the electron motion caused by an angle between the gauge axis and the magnetic field. First, there is a reduction on the acceleration rate, due to the parallel component of the electric field being

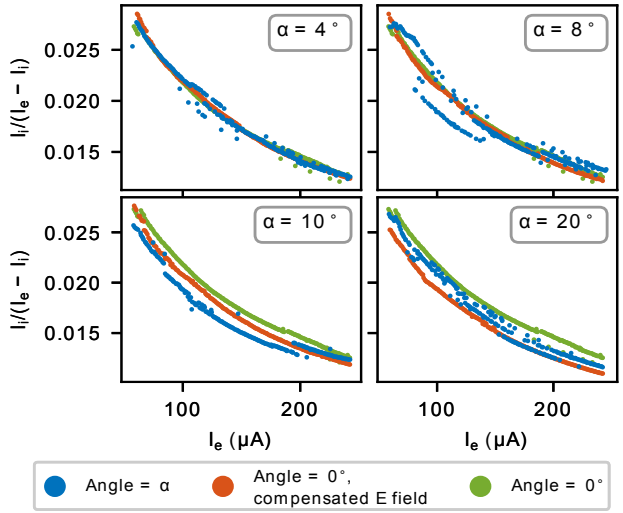

Figure 10: Normalized ion current as function of I_e for multiple angles of the gauge respect to the magnetic field during electron current ramps, as well as reference measurements at $\alpha = 0°$ both with equal and compensated electric field.

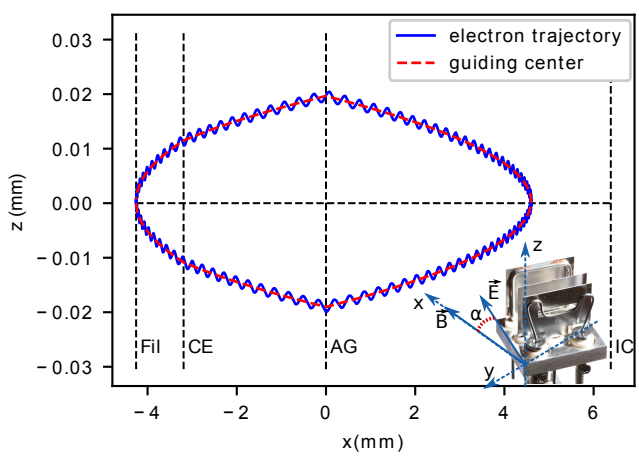

Figure 11: Simple simulation of an electron trajectory with angle $\alpha = 20°$ between electric $\vec{E}$ and magnetic field $\vec{B}$, influenced by ExB drift. Depiction of the direction of rotation of the gauge respect to the field in the lower right corner. The magnetic field is chosen to be parallel to the x axis and both electric and magnetic fields lie in the x-y plane.

reduced. Second, there is the possibility that an ExB drift changes the motion of the electrons. To test whether the difference observed could be explained by the reduction of the parallel electric field alone, reference measurements were taken with no angle and with adjusted electrode potentials so that the electric field would be equal to the parallel component at each value of the angle. This reference measurement are represented in red in Fig. 10. The compensation of the electric field results in decreased amount of ionization, which is to be expected since the electrons have less kinetic energy. The result from these experiments is that the behaviour of the jump changes significantly when a magnetic field angle is introduced with respect to reference measurements at 0° even if the electrode potentials are adjusted to compensate for the reduced electric field. This suggests that the $E \times B$ force role plays a role in the electron motion. Fig. 11 shows a 2D projection of the electron trajectory when the $E \times B$ drift is taken into account. The total drifts cancels over one oscillation period, but it can reach values of 0.04 mm at the AG. The drift distance is small compared with AG slit spacing (0.4 mm), but it is significantly larger than the gyration radius of the the electrons.

The effect of the $E \times B$ drift was discussed in Ref. [7], which predict an influence of the $E \times B$ drift on the electron trajectory even with parallel magnetic field, due to inhomogeneity in the electric field, based on single particle Monte-Carlo simulations.

2.4. Internal parameter space exploration

In order to explore which combination of the internal parameter minimizes the occurrence of the jumps, systematic test sets were carried out consisting each of up to 30 I_{e} ramps. Each measurement in a set was done with incremental changes of either V_{AG} or V_{CE}, while the other potential was constant. A different value of pressure was used for each set of measurements so that the results were not only valid for a given value.

In order to measure the jump occurrence rate, an automated routine to detect the jumps was necessary. This routine counts a jump when there is a

sudden variation on the ion current higher than a threshold of 1.5% of the total current. It has the limitation of only being able to detect one jump per time window of 5.25 ms. Therefore, the maximum occurrence rate measurable with this method is $190.5\,\mathrm{s}^{-1}$.

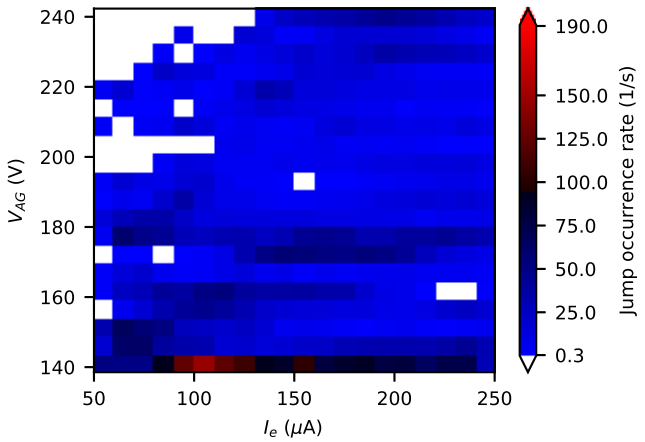

Figure 12: 2D histograms of jump occurrence rate over V_{AG} and I_{e} parameter space. V_{CE}= 135.3 V.

Fig. 12 shows a 2D histogram of the occurrence rate of the jump as a function of the electron current and the AG potential. The data from 6 of the measurements sets previously described is represented. A CE potential of 135.3 V was used for all of these measurements, and 6 different values of pressure were used in the range $2.0\times10^{-4}-8.86\times10^{-3}$ mbar. The white area represents the regions of the parameter space in which no jumps were detected. The amount of measurement time represented by a square in the histogram is 3.0 s. Therefore, the white area indicates a jump occurrence rate smaller than $0.33\,\mathrm{s}^{-1}$. It can be observed that some regions present higher occurrence rates, but the occurrence of the jumps is distributed across most of the parameter space, with few areas in which no jumps were detected at all.

Fig. 13 shows a 2D histogram constructed with the same method for the parameter space of V_{CE} and I_{e}. The data represented results from 4 measurement sets. V_{AG} is set to 241.8 V for all of the measurements, with pressures in the

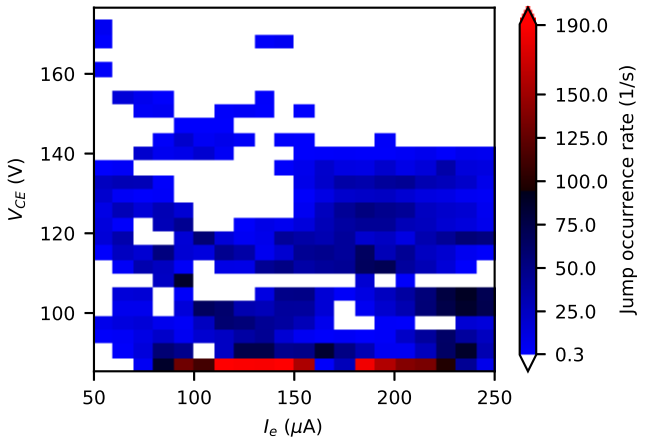

Figure 13: 2D histograms of jump occurrence rate over V_{CE} and I_{e} parameter space. V_{AG}= 241.8 V.

range $2.5\times10^{-4}-1.81\times10^{-3}$ mbar.

2.5. Optimal internal parameters to minimize current jumps

In the parameter space represented in Fig. 13, there is a region for I_{e} larger than 150 µA and V_{CE} larger than 150 V in which no jumps were detected. This result provides a combination of internal parameters that would minimize the jumps. However, this should be taken only as an approximate results, since it could be to some degree specific to the individual gauge used for the experiments. Also, the lack of long-term reproducibility of the jumps due to changes in the filament surface means that the point in the parameter space at which each individual experiences jumps may change over its operation life.

The exploration of the parameter range for V_{AG} did not reveal any range of values at which the jump occurrence rate is significantly reduced. Therefore, the use of its current value at 250 V is advised, since it is sufficiently close to the value of 241.8 V that was used for the test of the V_{CE} parameter range.

Taking this into account, the combination of internal parameters from table 1 is suggested for future operation of the gauges.

Table 1: Electrode positions and optimal voltage configuration for jump frequency reduction.

	x (mm)	Voltage (V)	Electric field (kV/m)
Fil.	-4.0	70	-85
CE	-3.0	155	-32
AG	0.0	250	42
IC	6.0	0	-

3. Possible causes of the jumps

From the results presented so far, it is clear that the underlying process responsible for the jumps is a change in the electron motion due to electron-to-electron interaction, leading to a change in the confinement of the electrons. A change in the electron confinement would explain the modified value of I_i once I_e has returned to its normal value. It is important to consider the electrons which are reabsorbed at the filament, and therefore do not contribute to I_e. Changes in the electron motion could cause a change in the fraction of lost electrons by reabsorbtion.

The dependency of the ion current jumps with the electron current suggests that the electron density is one of the parameters that causes this change in electron motion. This is also supported by the detection of electron current spikes at low pressures where the ions do not play a role, and by the disappearance of the jumps at higher pressures, described in subsection 2.3. The pressure is linked to the amount of electron-neutral collisions, and, therefore, it regulates how many electrons are trapped oscillating back and forth the AG, and for how long do the electrons remain in the system until they lose all their kinetic energy. For reference, at a pressure of 6×10^{-2} mbar, near the maximum value at which jumps are detected, I_i is 72.6 µA for an electron current of I_e of 200 µA. In this case, it is clear that the fraction of electrons that collide with neutrals is significant, thus influencing the electron density. The high pressure operation of the ASDEX gauges and the fraction of electron-neutral collisions is discussed in Ref. [8]. The ionization events also produce secondary electrons, which add to the total electron density. At higher pressures the electron collide with neutrals

more often, leading to a decrease in the time they are present in the system before they are absorbed at the AG, and thus, a decrease in electron-to-electron interaction.

The underlying mechanisms of the current jumps need to explain the four possible combinations of directionality in the changes in I_e and I_i. Two possible scenarios are proposed:

- **Sudden change in the electron energy distribution**: a sudden widening of the parallel energy distribution of the electrons would result in an increased fraction of trapped electrons, as more electron would lose part of their kinetic energy and become confined, and less electrons would be reabsorbed at the filament and lost. Thus, I_e would increase as more electrons would eventually reach the AG. At the same time, the average energy per electron would have been decreased, as the confined electrons have lost kinetic energy to the lost electrons. Therefore, I_i would decrease. The reverse, the narrowing of an already wide distribution, would result in a decrease of I_e and an increase of I_i.

- **Change in electron confinement**: a change in the fraction of lost electrons without a significant change in the electron energy distribution would result in a change of I_i and I_e in the same direction.

This section discusses possible physical mechanism in which electron-to-electron interaction would lead to one of these scenarios and the experiments done to test them.

3.1. Space charge effects

One possible cause of the jumps is the interaction of the electrons with an inhomogeneous electric field due to the presence of an electron space charge. This would create a potentially unstable feedback relationship between the electron current, which would be influenced by the electron density, and in turn, would also influence the electron density. As already discussed, the $E \times B$ forces

can play a role in the electron motion. An inhomogeneous electric field would amplify this effect, decreasing the confinement of the electrons.

In experiments with thermionic electron emission from a biased filament, space charge effects have been known to play a role. In Ref. [9], R. Timm and A. Piel describe current jumps in thermionic discharges. They describe two different states of electron emission, one of them regulated by the presence of negative space charge, and current jumps in between the two states, following a hysteresis cycle. Even though there are differences in the dimensions of their experiment and the ionization gauges, the similarities were enough to consider this as a possible explanation for the jumps.

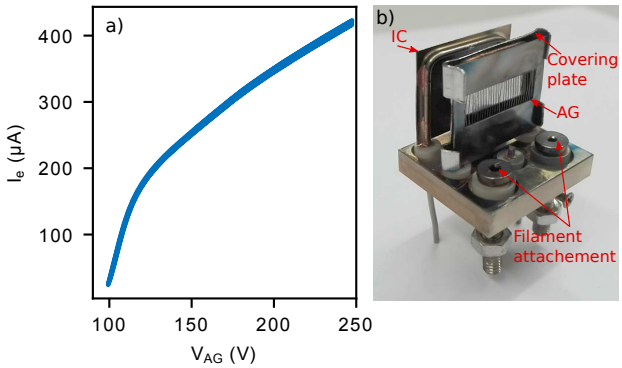

Figure 14: Electron current as function of V_{AG} during four cycles of increasing and decreasing voltage between 100 V and 250 V when the AG was covered by a metal plate (a). Picture of the modified gauge (b).

To test for this scenario, a pressure gauge was modified with a metal plate behind the AG, shown in Fig.14 (b). The metal plate function is to absorb the electrons after they pass through the AG, and thus prevent the counter-streaming motion. The CE was removed to further simplify the system. With this setup, repeating cycles of increasing and decreasing V_{AG} were performed in order to try replicating the jumps and hysteresis reported in Ref. [9]. As can be seen in Fig. 14 (a), the current experiences no jumps. This shows that the space charge limited extraction is not responsible for the jumps, at least in the tested parameter space. The fact that the current to voltage curve has a positive slope

shows that the emission from the filament is being limited by the presence of space charge. Repeating the experiments with the same gauge with the metal plate removed produced current jumps.

These results indicate that, while there is presence of space-charge in the system, this alone is not the cause of the jumps. The space-charge distribution should be taken into account to better understand the electron motion. Another result is that the counter-streaming electron motion is necessary for the jumps to happen in the tested parameter range.

3.2. Counter-streaming electron beam instabilities

Since the jumps are only observed when there is counter-streaming electron motion, possible explanations for the current jumps are the two-stream instability, and the half-cyclotron-frequency instability. Both are instabilities that can arise when there are two populations of charge particles moving in opposite directions, and can result in kinetic energy transfer between electrons. A non-linear change of the electron velocity distribution could result in sudden change in the survivability of the electrons, resulting in spikes in the electron current, which consequently cause jumps in the ion current. Since the cross-section of ionization is dependent on electron velocity, the change in the electron velocity distribution could explain why the I_i and I_e jumps are not proportional in amplitude.

The two-stream instability has been reported in Ref. [10] in experiments with similar parameters to the ones in the pressure gauges. In these experiments, an unstable mode is excited when an electron beam enters an stationary plasma which acts as the opposing electron population. The point at which the unstable mode is exited is dependent on the electron velocity.

The other candidate is the half-cyclotron-frequency instability. It has been reported in experiments with counter-streaming electron beams in the presence of a magnetic field in Refs. [11] and [12]. As the name implies, it is associated with an unstable mode with a frequency equal to half the electron gyration frequency.

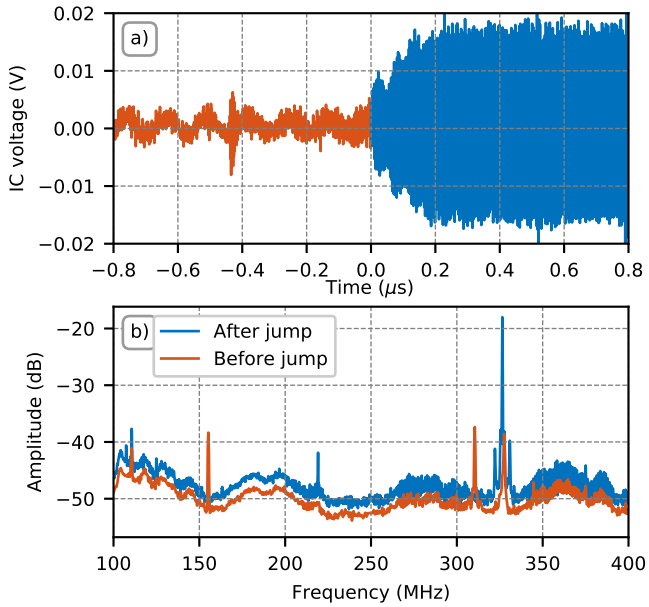

Figure 15: Oscilloscope measurement during which a jumps occurs at $t = 0\,\mathrm{s}$ (a). Fourier transform of the measurement before and after the jump (b).

In order to detect the electromagnetic oscillations associated with these instabilities, experiments were done while using the ion collector plate as an antenna and connecting it to a high frequency oscilloscope (Lecroy Waverruner 204Xi [13]), with up to 5 GHz sampling rate. A continuous V_{CE} was used to avoid interference created by the chopping cycles in the measurements. Other channels of the oscilloscope were connected to voltages proportional to I_{e} and I_{i} so that the measurement could be triggered before or after a jump occurs.

Fig. 15 shows one oscilloscope measurement which was triggered at the exact moment a jump happened. The amplitude of the oscillations significantly increases after the moment of the jump at $t = 0\,\mathrm{s}$. Frequency analysis of the oscillations reveal frequency peaks that change in amplitude after a jump occurs. Multiple measurements were taken with different electrode potential configurations with two different gauges.

The comparison of the frequency analysis before and after the jump shows that the jumps influence the detected frequency spectra. The number of peaks

change in different measurements. The general behavior is that there is at least one low frequency peak (157 MHz in the example in Fig. 15), which disappears after the jump and there is at least one frequency peak with significantly higher amplitude after the jump appears or increases in amplitude after the jump (327 MHz in this example). These peaks are only present while there is electron emission. Fig 18 in the appendix shows a comparison of another measurement and the background noise, measured without electron emission. In this comparison it is possible to appreciate the complex structure of the frequency peaks, including the higher harmonics.

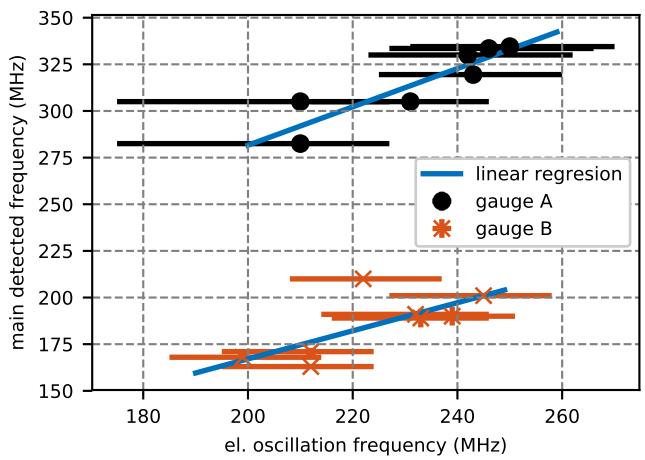

Figure 16: Correlation between main detected frequency after jumps and electron oscillation frequency with different electrode potentials configurations, for two different gauges. The error bars account for a systematic error of ± 1.0 mm in the measurement of the gauge dimensions.

The value of the main frequency detected after the jumps was found to scale with the oscillation frequency of the electrons back and forth the AG, as represented in Fig. 16. The oscillation frequency of the electrons is dependent on the electrode potential configuration. Different combinations of V_{AG} and V_{CE} were used with two different gauges. For each of the gauges, the detected frequency appears to follow an approximately linear trend with the electron oscillation frequency. The slope of the linear regression is 1.02 ± 0.22 for gauge A, and 0.75 ± 0.30 for gauge B. The additive constants are (76 ± 52) MHz for A, and (16 ± 68) MHz for B. These values are within the error margin of being a

1 to 1 correspondence between main detected frequency and electron oscillation frequency.

The detected frequency does not scale with the magnetic flux density, as would be expected if it was associated with the half-cyclotron-frequency instability. The experiments were repeated with magnetic flux densities in the range of $0.002 - 0.8\,\mathrm{T}$ and no change in the detected frequencies was observed, which rules out this possibility.

The two stream instability remains a possible hypothesis, since the detected frequency scales with the velocity of the electrons, which is modified when the electrode potentials are changed. But the similarity of the measured frequency with the electron oscillation frequency could also suggest some other mechanism, such as coherent oscillation of electrons due to bunching.

Experiments were also done to measure the energy distribution of the electrons. To this end, the bias voltage of the filament was set to $0\,\mathrm{V}$ and gradually increased. The current of electrons is measured in the IC plate, which now the electrons can reach since it is at the same potential as the filament. As the bias voltage is increased, the fraction of electrons that can reach the IC correspond to electrons which have been emitted with or have gained sufficient energy to overcome the potential difference. When the potential difference is $0\,\mathrm{V}$, all electrons would be able to reach the plate if no kinetic energy is lost. Under that assumption, the energy distribution of the electrons parallel to $\vec{B}$ is measured. However, for a better measurement, the fraction of electrons which lost energy should also have been taken into account by decreasing the filament bias below zero.

The curves of the electron parallel energy distributions are shown in Fig.17 for different values of I_e as measured in the AG. The electron temperature T_e can be calculated by fitting the curves with a cumulative Maxwell-Boltzmann distribution. As it can be observed, even at low I_e values, the electron temperature is significantly higher than the filament temperature of around $1800\,\mathrm{K}$. This proves that there is a mechanism that allows momentum transfer between

electrons so that their energy distribution is widened further than their emission temperature.

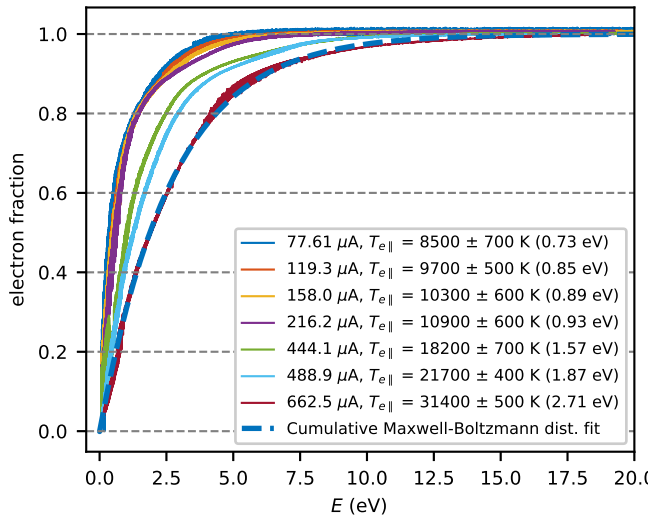

Figure 17: Fraction of electrons with kinetic energy (parallel to magnetic field) smaller or equal than E, for different values of I_e. The dashed line represents an example for the cumulative Maxwell-Boltzmann distribution fit used to estimate the electron parallel temperature.

4. Conclusions

The ion current jumps which first had been seen in gauges installed in ASDEX Upgrade and W7-X, were successfully reproduced in the laboratory, and their occurrence has been explored over a wide parameter range. This revealed an upper limit of the pressure at which jumps appear of 6.7×10^{-2} mbar, while no lower limit was found above the lowest reachable pressure of 10^{-8} mbar, and an optimal internal parameter combination ($V_{\mathrm{fil}} = 70\,\mathrm{V}$, $V_{\mathrm{CE}} = 155\,\mathrm{V}$, $V_{\mathrm{AG}} = 250\,\mathrm{V}$, and $I_{\mathrm{e}} = 200\,\mu\mathrm{A}$) to minimize the jumps.

The experimental evidences indicates that the jumps are a result of collective behaviour of the electrons as a result of their counter-streaming motion. The appearance of perturbations in I_{e} in vacuum proves that the ions are not necessary for the jumps to occur, and rules out the discrete ionization energies of the neutral gas molecules as a possible cause. The parameter dependencies

discussed suggest the electron density is a predominant factor for the jumps, since the electron density is influenced by the total electron current and the neutral gas pressure.

The exact mechanism by which the jumps take place remains unclear. However, the experiments prove that there is significant momentum transfer between electrons. This indicates the presence of electron collective behavior. The appearance or substantial increase in amplitude of electromagnetic oscillations has been proved to be related to the jumps. The change in these oscillations occurs simultaneously with the current jumps, and their nature is subject for further studies to find the ultimate cause of the current jumps. For this end, simulations that take electron-to-electron interactions into account could be useful, but are beyond the scope of this work.

Acknowledgments

Colleagues Sofía Díaz Esteban and Markus Wappl are thanked for their help and discussions.

This work has been carried out within the framework of the EUROfusion consortium and has received funding from the Euratom research and training programme 2014-2018 and 2019-2020 under grant agreement No 633053. The views and opinions expressed herein do not necessarily reflect those of the European Commission.

Data Availability

The data that support the findings of this study includes raw data form the ASDEX Upgrade facility and data from laboratory experiments, which is available from the corresponding author upon reasonable request.

Conflict of Interest Statement

The authors have no conflicts to disclose.

References

[1] G. Haas, H.-S. Bosch, In vessel pressure measurement in nuclear fusion experiments with asdex gauges, Vacuum 51 (1) (1998) 39 – 46. doi:https://doi.org/10.1016/S0042-207X(98)00131-6.
URL http://www.sciencedirect.com/science/article/pii/S0042207X98001316

[2] U. Wenzel, T. Kremeyer, G. Schlisio, M. Marquardt, T. Pedersen, O. Schmitz, B. Mackie, J. M.-B. and, Advanced neutral gas diagnostics for magnetic confinement devices, Journal of Instrumentation 12 (09) (2017) C09008–C09008. doi:10.1088/1748-0221/12/09/c09008.
URL https://doi.org/10.1088/1748-0221/12/09/c09008

[3] A. Arkhipov, F. Mackel, A. Scarabosio, G. Haas, J. Koll, H. Eixenberger, H. Meister, F. Seyvet, S. Terron, P. Andrew, Progress in development of iter diagnostic pressure gauges and status of interfaces with iter components, Fusion Engineering and Design 146 (2019) 1262 – 1266, sI:SOFT-30. doi:https://doi.org/10.1016/j.fusengdes.2019.02.054.
URL http://www.sciencedirect.com/science/article/pii/S0920379619302303

[4] U. Wenzel, G. Schlisio, M. Mulsow, T. S. Pedersen, M. Singer, M. Marquardt, D. Pilopp, N. Rüter, Performance of new crystal cathode pressure gauges for long-pulse operation in the wendelstein 7-x stellarator, Review of Scientific Instruments 90 (12) (2019) 123507. doi:10.1063/1.5121203.

[5] F. Mackel, A. Arkhipov, A. Scarabosio, G. Haas, J. Koll, H. Meister, F. Seyvet, S. Terron, P. Andrew, Experimental exploration of the upper measuring limit of pressure gauges for iter by variation of instrumental parameters, Fusion Engineering and Design 146 (2019) 622–625, sI:SOFT-30. doi:https://doi.org/10.1016/j.fusengdes.2019.01.038.
URL https://www.sciencedirect.com/science/article/pii/S092037961930047X

[6] K. Jousten, P. Röhl, Instability of the spatial electron current distribution in hot cathode ionization gauges as a source of sensitivity changes, Journal of Vacuum Science & Technology A 13 (4) (1995) 2266–2270. arXiv:https://doi.org/10.1116/1.579506, doi:10.1116/1.579506.
URL https://doi.org/10.1116/1.579506

[7] A. Scarabosio, P. Sauter, G. Haas, Modelling and optimisation of ionisation gauges for magnetic nuclear devices, Nuclear Instruments and Methods in Physics Research Section A: Accelerators, Spectrometers, Detectors and Associated Equipment 623 (2) (2010) 667–671, 1rs International Conference on Frontiers in Diagnostics Technologies. doi:https://doi.org/10.1016/j.nima.2010.02.258.
URL https://www.sciencedirect.com/science/article/pii/S0168900210005437

[8] A. Scarabosio, G. Haas, Behaviour of the asdex pressure gauge at high neutral gas pressure and applications for iter, AIP Conference Proceedings 988 (1) (2008) 238–242. arXiv:https://aip.scitation.org/doi/pdf/10.1063/1.2905075, doi:10.1063/1.2905075.
URL https://aip.scitation.org/doi/abs/10.1063/1.2905075

[9] R. Timm, A. Piel, Hysteresis and transition to chaos in a themionic plasma discharge, Contrib. Plasma Phys. 32 (6) (1992) 599–611.

[10] V. Fedorchenko, B. Rutkevich, V. Muratov, Non-linear limitation of double-stream instability, Nuclear Fusion 11 (1) (1971) 43–50. doi:10.1088/0029-5515/11/1/006.
URL https://doi.org/10.1088/0029-5515/11/1/006

[11] A. Hershcovitch, P. A. Politzer, Time evolution of velocity-space instabilities on counterstreaming, magnetically confined electron beams, Physical review letters 36 (1976) 1365–1368.

[12] M. Murakami, L. M. Lidsky, Growth and damping of wave-particle inter-

actions in counterstreaming electron beams, Physical review letters 24 (7) (1970) 297–300.

[13] Lecroy waverrunner xi-series oscilloscopes manual, `http://cdn.teledynelecroy.com/files/manuals/wrxi_om_revc.pdf`, accessed: 2021-11-01.

Appendix

Table 2: Tested parameter range of internal and external parameters of gauge operation.

	Parameter range	Increment steps
I_e (µA)	$40-500$	continuous
pressure (mbar)	$10^{-8}-6.0\times10^{-1}$	$5\times10^{-5}-5\times10^{-2}$
V_{AG} (V)	$145-250$	3
V_{CE} (V)	$94-184$	2.5
field angle	$-20-20°$	2°

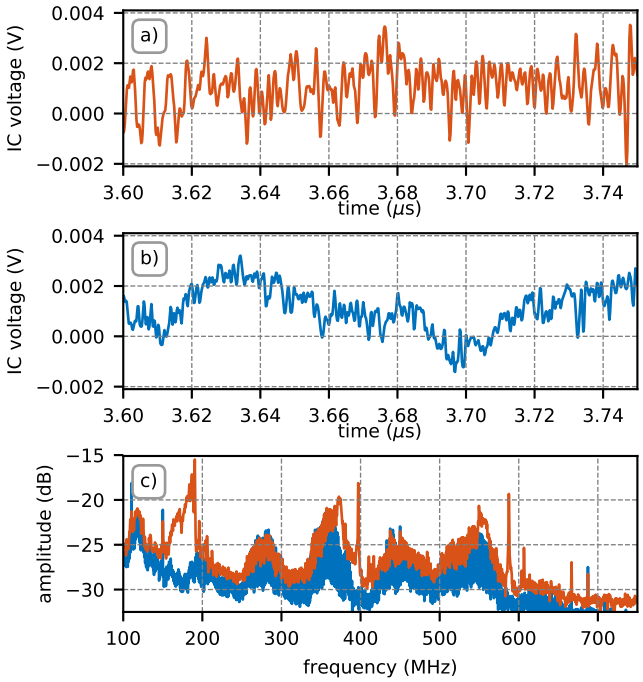

Figure 18: Portion of oscilloscope measurement of IC voltage after jump (a). Portion of oscilloscope measurement of background noise with no electron emission (b). The full measurements last 0.2 ms. (c) is the frequency analysis of the measurement after a jump (red) and the background noise (blue).